

CORRECTION TO: SPATIOTEMPORAL WILDFIRE MODELING THROUGH POINT PROCESSES WITH MODERATE AND EXTREME MARKS

BY JONATHAN KOH^{1,2,a}, FRANÇOIS PIMONT^{3,b}, JEAN-LUC DUPUY^{3,c} AND THOMAS OPITZ^{4,d}

¹Institute of Mathematics, EPFL

²Institute of Mathematical Statistics and Actuarial Science, Oeschger Centre for Climate Change Research, University of Bern, ^ajonathan.koh@unibe.ch

³URFM UR629, INRAE, ^bfrancois.pimont@inrae.fr, ^cjean-luc.dupuy@inrae.fr

⁴BioSP UR546, INRAE, ^dthomas.opitz@inrae.fr

1. Figures. Due to an error during the production process, Figure 2 was not included in Koh et al., 2023. Subsequently, the remaining figures do not appear in the proper place. Following are all figures as they should have appeared.

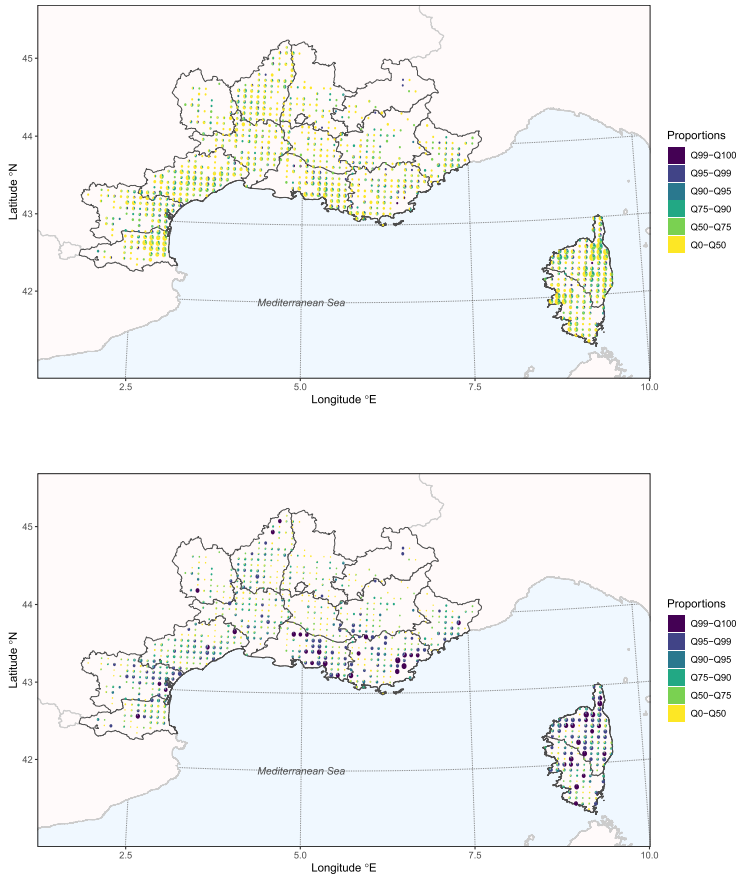


FIG. 1. Maps of Prométhée data aggregated to the SAFRAN grid at 8 km resolution. The pie charts in the grid cells are based on 1 wildfire size classes with boundaries given by empirical quantile levels 0, 0.5, 0.75, 0.9, 0.95, 0.99, 1 of all burnt areas (June–October). Top display: Pie charts show relative count proportions over the six classes and have size increasing with increasing counts. Bottom display: Pie charts show relative burnt area proportions and have size increasing with increasing aggregated burnt area.

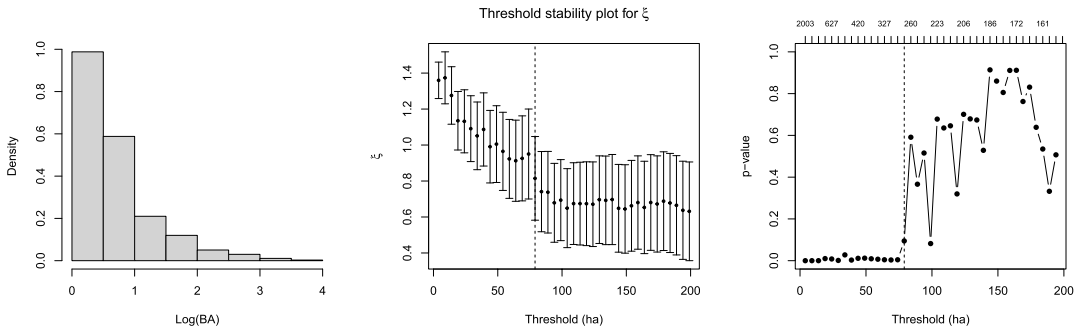


FIG. 2. Burnt area distribution. Left: Histogram of burnt areas (ha) in base-10-logarithm. Middle: Parameter stability of the tail index. Right: P-values for the null hypothesis of a GPD distribution above the threshold; tick labels on top indicate the number of fires above the thresholds.

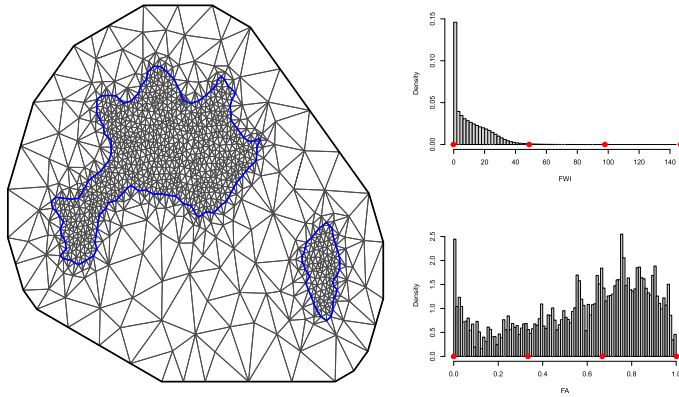


FIG. 3. Discretization of random effects with SPDE-based Gaussian prior processes. Left: Triangulation mesh of the study area (blue contours) for the SPDE approach. Neumann boundary conditions are set on the exterior (black) boundary to obtain a unique solution. The finite element solution defines a Gauss–Markov random vector with one variable in each node. Right: Histograms of FWI and FA values. The red points indicate where the spline knots are placed.

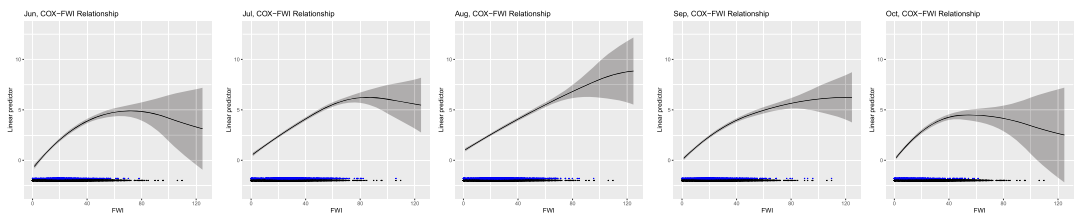


FIG. 4. Posterior estimates of $g_3^{\text{COX}}(\cdot; m) + g_5^{\text{COX}}(m)$, $m = 1, \dots, 5$, the joint FWI-month effect, for June–October in the linear predictor of the point process (COX) component. The blanket of black and blue points at the bottom of each plot shows FWI values for pixel-days with fires in any month and the specific month, respectively.

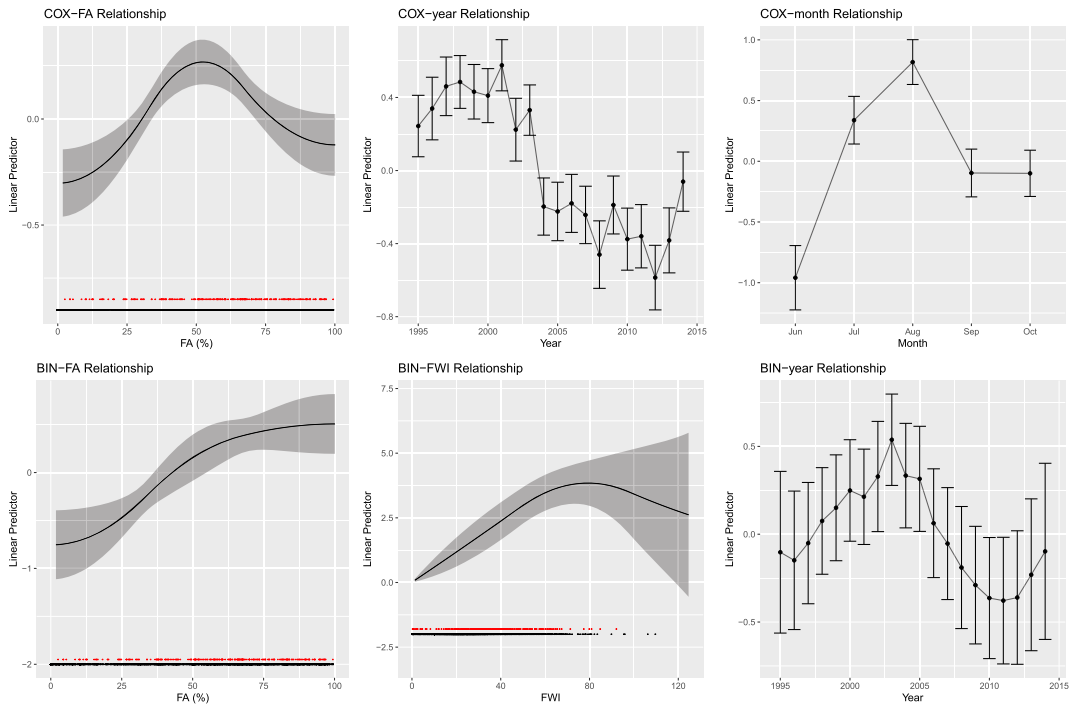


FIG. 5. Posterior estimates of $g_2^{\text{COX}}(\cdot)$ (FA effect, top left panel), $g_4^{\text{COX}}(\cdot)$ (year effect, top middle panel), $g_5^{\text{COX}}(\cdot)$ (month effect, top right panel), $g_2^{\text{BIN}}(\cdot)$ (FA effect, bottom left panel), $g_1^{\text{BIN}}(\cdot)$ (FWI effect, bottom middle panel) and $g_3^{\text{BIN}}(\cdot)$ (year effect, bottom right panel) in the linear predictor of the point process (COX) component and large wildfire probability component (BIN). At the bottom of some displays, the blanket of black and red points shows FA/FWI values for pixel-days with moderate and large fires, respectively.

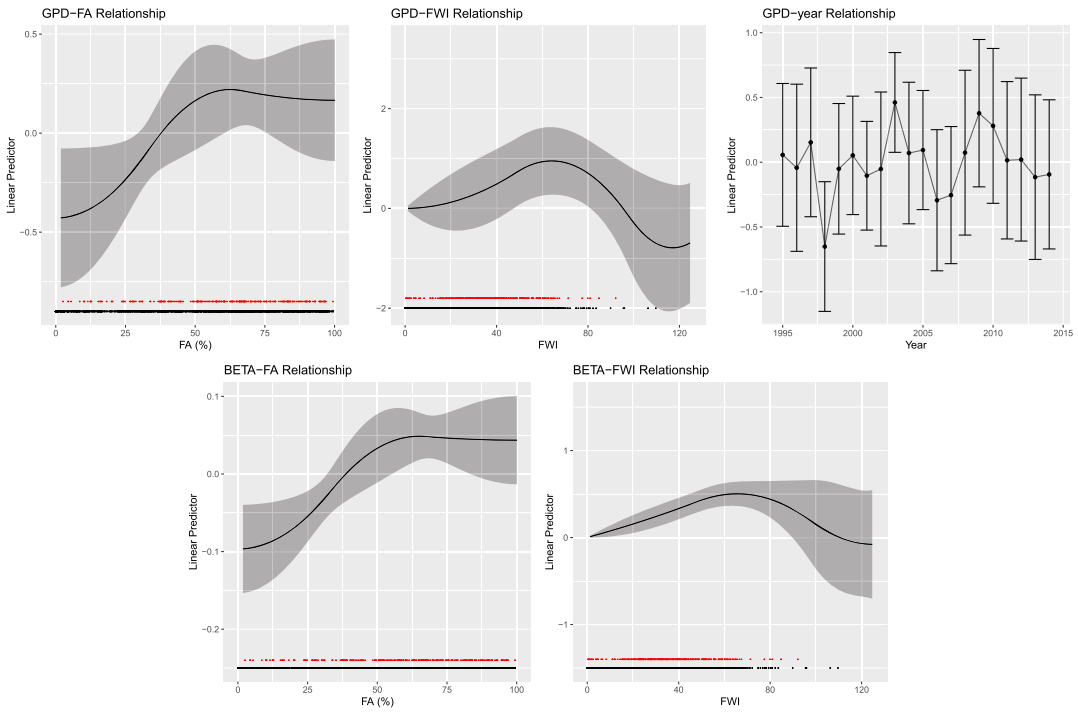


FIG. 6. Panels as in Figure 5. Posterior estimates of $g_2^{\text{GPD}}(\bullet)$ (FA effect, top left), $g_1^{\text{GPD}}(\bullet)$ (FWI effect, top middle), $g_3^{\text{GPD}}(\bullet)$ (year effect, top right), $g_2^{\text{BETA}}(\bullet)$ (FA effect, bottom left) and $g_1^{\text{BETA}}(\bullet)$ (FWI effect, bottom right) in the linear predictor of the large wildfire size component (GPD) and moderate wildfire size component (BETA).

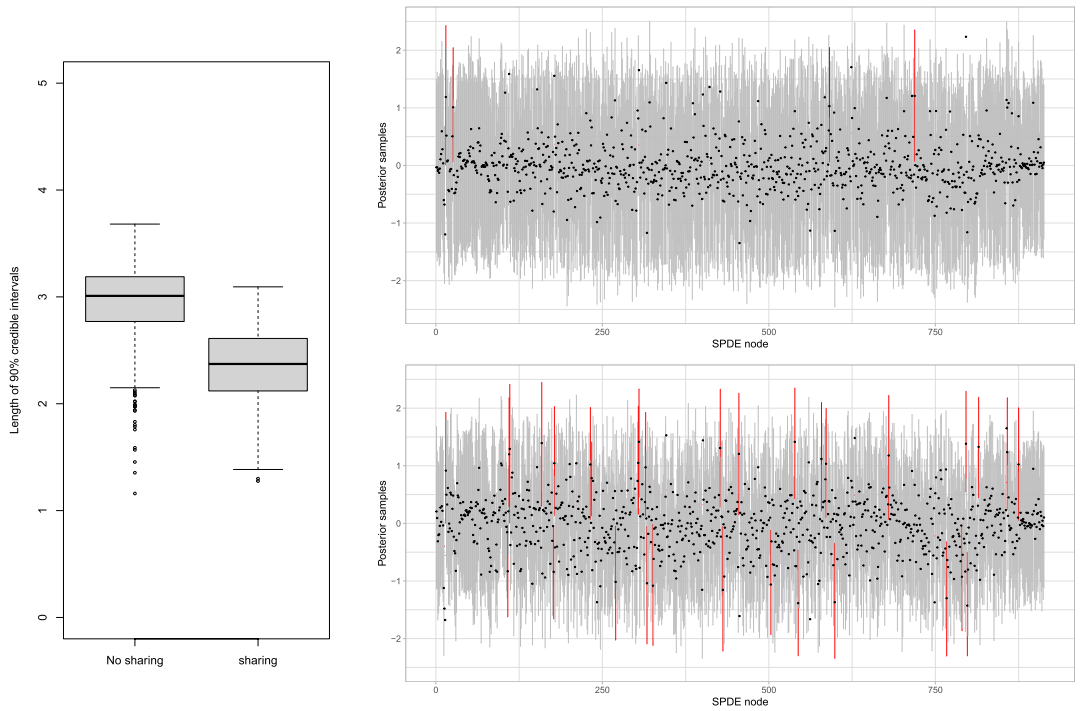


FIG. 7. Lengths of the 90% credible intervals of spatial random effect variables at the SPDE triangulation nodes within the study area in the BIN component, based on 500 posterior simulations. Boxplots (left) and error bar plots for the models without (top right) and with sharing (bottom right). Red error bars indicate nodes where the intervals do not include zero.

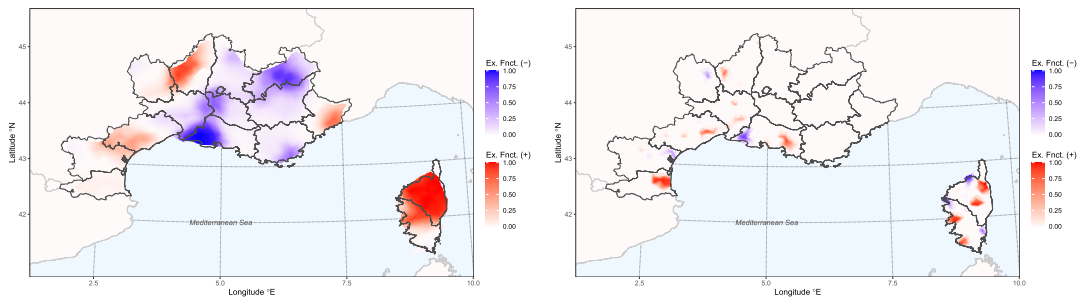


FIG. 8. Excursion functions of posterior latent fields above 0.1 and below -0.1 . Plots show $\max\{F_{0.1}^+(\cdot), F_{0.1}^-(\cdot)\}$ for the shared spatial random fields $g^{\text{COX-BETA}}$ (left panel) and $g^{\text{COX-BIN}}$ (right panel).

REFERENCES

- KOH, J., PIMONT, F., DUPUY, J.-L. and OPITZ, T. (2023). Spatiotemporal wildfire modeling through point processes with moderate and extreme marks. *Ann. Appl. Stat.* **17** 560–582. MR4539044 <https://doi.org/10.1214/22-aos1642>